

Perfluorinated Trialkoxysilanol with Dramatically Increased Brønsted Acidity

Felix Feige,^[a] Lorraine A. Malaspina,^[b] Elena Rychagova,^[c] Sergey Ketkov,^{*,[c]}
Simon Grabowsky,^{*,[b]} Emanuel Hupf,^{*,[a]} and Jens Beckmann^{*,[a]}

Dedicated to Professor Glen B. Deacon on the occasion of his 85th birthday

Abstract: The Brønsted acidity of the perfluorinated trialkoxysilanol $\{(F_3C)_3CO\}_3SiOH$ is more than 13 orders of magnitude higher than that of orthosilicic acid, $Si(OH)_4$, and even more for most previously known silanols. It is easily deprotonated by simple amines and pyridines to give the conjugate silanolates $[OSi\{OC(CF_3)_3\}_3]^-$, which possess extremely short Si–O bonds, comparable to those of silanones.

Orthosilicic acid, $Si(OH)_4$, is a very weak Brønsted acid.^[1] The same holds true for organosilanols, $R_nSi(OH)_{4-n}$, and alkoxy-silanols, $(RO)_nSi(OH)_{4-n}$ ($n=1-3$; R=alkyl, aryl), which can be regarded as organic derivatives or partial esters of $Si(OH)_4$.^[2] Like orthosilicic acid, most small organosilanols and alkoxy-silanols are sensitive towards self-condensation to give siloxanes and silica consisting of 2D or 3D networks of Si–O–Si linkages, which is of technical relevance for the curing of silicone resins and the sol-gel process.^[3] The self-condensation is accelerated by heat as well as traces of acid and base. However, self-condensation can be prevented by the judicious choice of mild reaction conditions and bulky substituents R, which allows the preparation of kinetically stabilized silanols that can be used for

synthetic purposes, such as the preparation of well-defined metallasiloxanes containing Si–O–M linkages.^[4] A prominent example is $(t\text{-BuO})_3SiOH$, which reacts with a variety of metals to give rise to thermolytic molecular precursors (TMPs) that upon heating produce multicomponent oxide materials, not accessible by the sol-gel process.^[5]

We have now set out to prepare a perfluorinated derivative of $(t\text{-BuO})_3SiOH$, which was achieved by two simple synthetic steps starting from commercially available starting materials. Thus, the reaction of $SiCl_4$ with three equivalents of $NaOC(CF_3)_3$ afforded $\{(F_3C)_3CO\}_3SiCl$ (**1**), the hydrolysis of which gave the silanol $\{(F_3C)_3CO\}_3SiOH$ (**2**) as low-melting crystals (Scheme 1).^[6] The key feature in the crystal structure of **2** is the isolated silanol group, which, unlike that of the parent $(t\text{-BuO})_3SiOH$,^[7] is not involved in hydrogen bonding (Figure 1).^[8] Due to the high charge separation in **2** associated with the large number of fluorine atoms, it possesses a dramatically increased Brønsted acidity, compared to orthosilicic acid $Si(OH)_4$ and all previously known silanol species (see below).^[9] For this reason, **2** can be readily deprotonated by weak and strong bases. Thus, the reaction of **2** with triethylamine, pyridine, lutidine and *n*-butyllithium provided the silanolates $[Et_3NH][OSi\{OC(CF_3)_3\}_3]$ (**3**), $[C_5H_5NH][OSi\{OC(CF_3)_3\}_3]$ (**4**), $[2,6\text{-Me}_2\text{C}_5\text{H}_3\text{NH}][OSi\{OC(CF_3)_3\}_3]$ (**5**) and $[Li(C_6H_4F_2)OSi\{OC(CF_3)_3\}_3]_2$ (**6**) that were isolated as crystalline solids (Scheme 2 and Figure 1).^[6]

The deprotonation of silanols by simple amines and pyridines is unprecedented.^[10] Usually, $Si(OH)_4$ ^[11] and all silanols are only known to form hydrogen-bonded complexes of the type $O\cdots H\cdots N$,^[12] which, for instance, has been utilized to build-up extended supramolecular networks.^[13] In **3** and **5**, the silanolate $[OSi\{OC(CF_3)_3\}_3]^-$ is associated with the triethylammonium ion, $[Et_3NH]^+$, and the lutidinium ion, $[2,6\text{-Me}_2\text{C}_5\text{H}_3\text{NH}]^+$, respectively, via a reverse, bipolar hydrogen bond of the type $^-O\cdots H\cdots N^+$ (Figure 1).^[14] The donor-acceptor distances in **3** (2.518(2) Å) and **5** (2.512(4) Å) are indicative of strong hydrogen bonding.^[12,15] This observation suggests that the silanolate $[OSi\{OC(CF_3)_3\}_3]^-$ is still rather basic, which is in clear contrast to

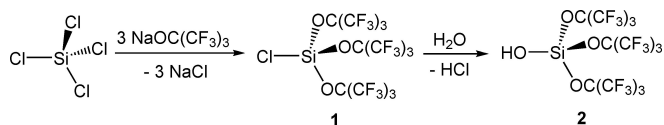
[a] F. Feige, Dr. E. Hupf, Prof. Dr. J. Beckmann
Institut für Anorganische Chemie und Kristallographie,
Universität Bremen
Leobener Straße 7, 28359 Bremen
(Germany)
E-mail: hupf@uni-bremen.de
j.beckmann@uni-bremen.de

[b] Dr. L. A. Malaspina, Dr. S. Grabowsky
Departement für Chemie, Biochemie und Pharmazie
Universität Bern
Freiestrasse 3, 3012 Bern (Schweiz)
E-mail: simon.grabowsky@unibe.ch

[c] Dr. E. Rychagova, Prof. Dr. S. Ketkov
G. A. Razuvaev Institute of Organometallic Chemistry RAS
49 Tropinin St., 603950 Nizhny Novgorod (Russian Federation)
E-mail: sketkov@iomc.ras.ru

Supporting information for this article is available on the WWW under
<https://doi.org/10.1002/chem.202103177>

© 2021 The Authors. Chemistry - A European Journal published by Wiley-VCH GmbH. This is an open access article under the terms of the Creative Commons Attribution Non-Commercial NoDerivs License, which permits use and distribution in any medium, provided the original work is properly cited, the use is non-commercial and no modifications or adaptations are made.



Scheme 1. Synthesis of $\{(F_3C)_3CO\}_3SiCl$ (**1**) and $\{(F_3C)_3CO\}_3SiOH$ (**2**).

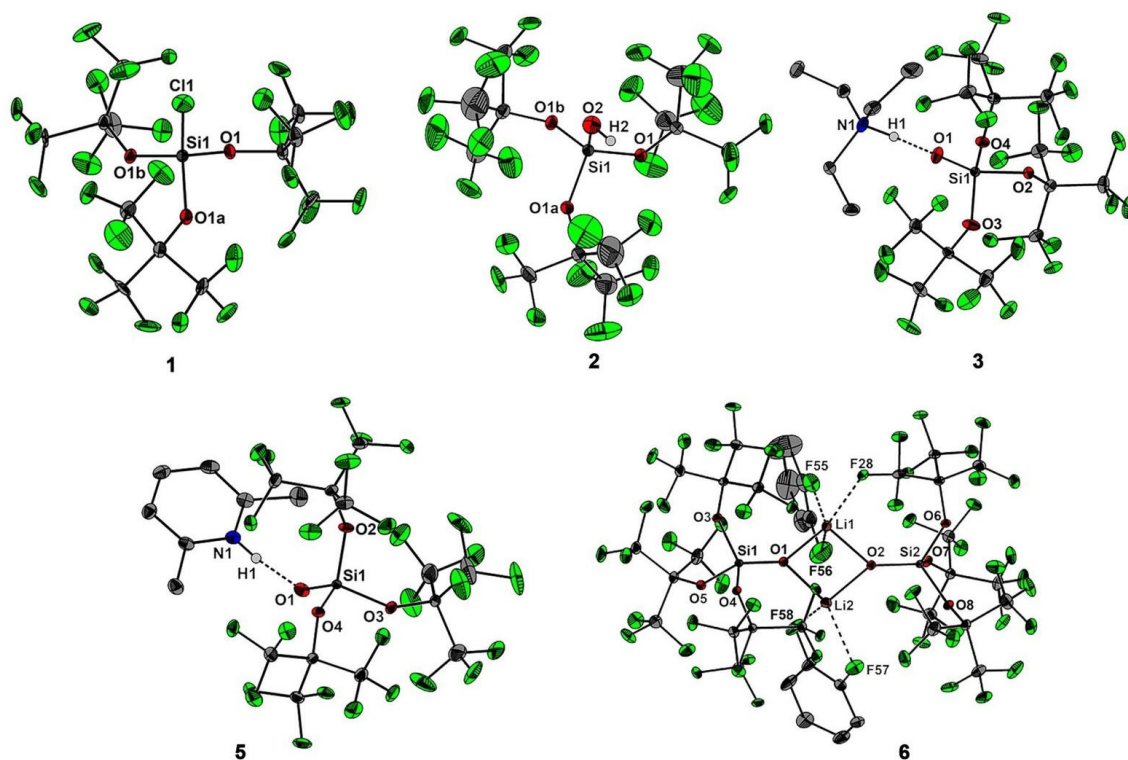
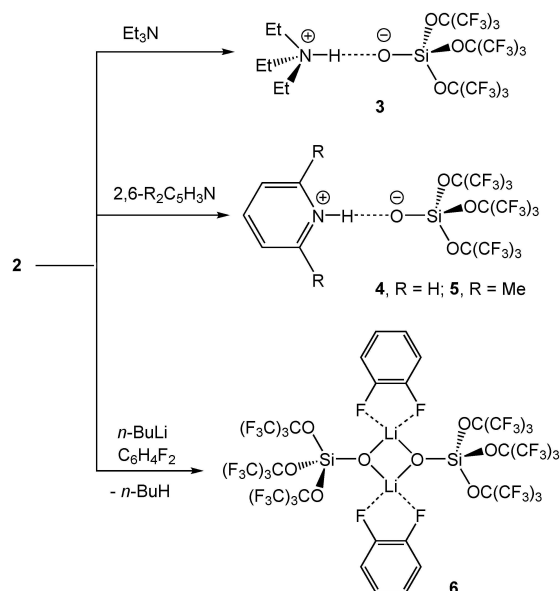


Figure 1. Molecular structures of 1–3, 5 and 6 from single-crystal X-ray diffraction. Selected bond distances [Å] of 1: Si1–O1 1.656(2), Si1–Cl1 1.981(4); of 2: Si1–O1 1.648(3), Si1–O2 1.621(12); of 3: Si1–O1 1.523(2), Si1–O2 1.653(1), Si1–O3 1.642(2), Si1–O4 1.649(1), O1...N1 2.518(2); of 5: Si1–O1 1.551(3), Si1–O2 1.630(3), Si1–O3 1.629(3), Si1–O4 1.639(2), O1...N1 2.512(4); of 6: Si1–O1 1.549(2), Si1–O3 1.636(2), Si1–O4 1.649(2), Si1–O5 1.643(2), Si2–O6 1.650(2), Si2–O7 1.631(2), Si2–O8 1.640(2), Li1–O1 1.844(4), Li1–O2 1.865(4), Li2–O1 1.890(4), Li2–O2 1.851(4), Li1...F28 2.127(5), Li1...F55 2.018(5), Li2...F56 2.133(4), Li2...F57 2.259(4), Li2...F58 2.080(4).



Scheme 2. Synthesis of the silanolate anions 3–6.

Krossing's isoelectronic fluoroaluminate $[\text{FAl}(\text{OC}(\text{CF}_3)_3)]^-$ that serves as a weakly coordinating anion (WCA).^[16] The Si–O(H) bond length of 2 (1.621(12) Å) falls in the range of $\text{Si}(\text{OH})_4$ (1.619(1), 1.626(1) Å),^[11] $(t\text{-BuO})_3\text{SiOH}$ (1.6154(10)/1.6155(10) Å,

see Supporting Information) and other silanols.^[2] In sharp contrast, the Si–O[−] bond lengths of the silanolate ions present in 3 (1.523(2) Å), 5 (1.551(3) Å) and 6 (1.549(2) and 1.551(2) Å) are significantly shorter and fall in the range usually observed for silanones (1.518(2) to 1.540(3) Å), formally possessing polarized double bonds that are best presented by bipolar $\text{Si}^+ \text{O}^-$ resonance structures.^[17]

In solution, 1 and 2 are characterized by ²⁹Si NMR chemical shifts (CDCl_3) of $\delta = -98.3$ and -109.1 ppm; the silanolate anions 3 ($\delta = -111.9$ ppm), 4 ($\delta = -109.7$ ppm) and 5 ($\delta = -112.5$ ppm) are slightly more shielded.^[18] The ¹H NMR spectrum (CDCl_3) of silanol 2 shows the acidic proton at $\delta = 3.86$ ppm. In the silanolate anions, the acidic proton, now attached to nitrogen, resonates at $\delta = 15.03$ (3), 13.22 (4) and 15.76 ppm (5), which is fully consistent with chemical shifts of other triethylammonium, pyridinium and lutidinium salts. The experimental acidity was determined using the Gutmann-Beckett method.^[19] The acceptor number (AN) of 2 (40.4) is significantly higher than that of Ph_3SiOH (31.3) and $(t\text{-BuO})_3\text{SiOH}$ (23.6).

Density functional theory (DFT) computations were conducted for the silanol 2 and the silanolate anions in 3, 5, 6 as well as for the free $[\text{OSi}(\text{OC}(\text{CF}_3)_3)_3]^-$ anion to analyse the O–H as well as the Si–O interactions by a complementary bonding analysis.^[20] Overall, the geometry optimized structures match those of the established experimental structures of 2, 3 and 6 well, with the exception of 5. Attempts to optimize 5 give rise

to a proton transfer and the formation of $[(F_3C)_3CO]_3SiOH \cdot NC_5H_3-2,6-Me_2$ ($2 \cdot NC_5H_3-2,6-Me_2$) comprising a neutral O—H...N hydrogen bond. Apparently, the presence of a bipolar hydrogen bond of the type $^-O \cdots H-N^+$ in **5** is restricted to an electric field as present in the crystal lattice. The difference to **3**, where the bipolar $^-O \cdots H-N^+$ hydrogen bond prevails also in isolation, can be explained by the substantially stronger basicity of triethylamine ($pK_b = 3.4$) as compared to lutidine ($pK_b = 7.4$).^[121] This difference can also be seen by the examination of the electron localizability indicator (ELI-D)^[222] and the non-covalent interaction (NCI) index.^[223] Selected ELI-D localization domains and NCI surfaces for silanol **2**, the amine complexes **3** and **5** as well as the free silanolate $[OSi\{OC(CF_3)_3\}_3]^-$ are shown in Figure 2. Comparing the monosynaptic $V_1(O)$ lone pair domains (shown in solid-yellow), a transition from a O—H bond in **2** (Figure 2a), over a N...H—O hydrogen bond in **5** (Figure 2b) to a N—H...O hydrogen bond in **3** (Figure 2c) is observed. Spatially complementary to the ELI-D is the NCI index (shown in transparent mode). In case of **5**, a red-coloured donut shaped area is observed along the N...H axis, which is absent in **3** giving further evidence of the silanolate type moiety also in the gas-phase. The O—H Wiberg bond index (WBI) of 0.26 and delocalization index (DI) of 0.25 in **3** further prove the significant weakening of the O—H bond, especially upon comparison to the silanol **2** (0.72/0.57) and the amine complex **5** (0.55/0.40) (Table 1).

Analysis of the O—H bond in the framework of the Atoms-In-Molecules^[24] methodology reveals no substantial differences in key parameters such as the electron density ($\rho(r)_{bcp}$) and its Laplacian ($\nabla^2\rho(r)$) at the bond-critical points (bcp) in silanols **2**, $HOSi(Ot-Bu)_3$ and the model compounds $HOSiH_3$, $HOSi(OH)_3$ and $HOSiF_3$ that would indicate a higher acidity of silanol **2** (ranging from $\rho(r)_{bcp} = 2.46$ to $2.49 \text{ e}\text{\AA}^{-3}$ and $(\nabla^2\rho(r))_{bcp} = -64.4$ to $-65.6 \text{ e}\text{\AA}^{-5}$ (Table S8)). In contrast, the Si—O(H) interaction is more influenced by the different substituents leading to higher ionic contributions for the silanol **2** and the model compound F_3SiOH as indicated by increased $G/\rho(r)_{bcp}$ values of 2.09 and 2.08 h e^{-1} , respectively, compared to 1.97 h e^{-1} for silanols $HOSi(Ot-Bu)_3$ and $HOSiH_3$. Interestingly, the $\rho(r)_{bcp}$ at the Si—O(H) bcp for $HOSi(Ot-Bu)_3$ of $0.93 \text{ e}\text{\AA}^{-3}$ is smaller than the $\rho(r)_{bcp}$ to the other three Si—O(C) bonds (av. $0.99 \text{ e}\text{\AA}^{-3}$), whereas the opposite trend is observed for silanol **2** (Si—O(H): $1.04 \text{ e}\text{\AA}^{-3}$; Si—O(C): av. $0.94 \text{ e}\text{\AA}^{-3}$) although the ionic/covalent contributions indicated

Table 1. Wiberg bond/delocalization indices (WBI / DI) corresponding to the Si—O, O—H and N—H interactions in silanols, silanolates and silanones.

Molecule ^[a]	Si—O	O—H	N—H
HO—SiR ₃ (2)	0.70/0.38	0.72/0.57	—
HO—Si(Ot-Bu) ₃	0.61/0.34	0.74/0.63	—
[2,6-Me ₂ C ₅ H ₃ N][HO—SiR ₃] (5)	0.76/0.42	0.55/0.40	0.17/0.16
[Et ₃ N—H][O—SiR ₃] (3)	0.86/0.47	0.26/0.25	0.47/0.39
[O—SiR ₃] [−]	1.15/0.60	—	—
[O—Si(Ot-Bu) ₃] [−]	0.97/0.52	—	—
R' ₂ Si ⁺ —O [−]	1.26/0.81	—	—

[a] R = OC(CF₃)₃; R'₂ = {C[C₆H₂(t-Bu)₂(OMe)]₂C₂H₄}.

by the $G/\rho(r)_{bcp}$ and $H/\rho(r)_{bcp}$ ratios are rather similar (Table S8). After proton abstraction, the silanolate moieties of complexes **3** and **6** lead to substantial differences in the Si—O/Si—O(C) bonding. The differences in electron density and its Laplacian at the bcp becomes more pronounced with $\rho(r)_{bcp}$ values of 1.16 to $1.17 \text{ e}\text{\AA}^{-3}$ (Si—O) and $0.86 \text{ e}\text{\AA}^{-3}$ (av. Si—O(C)). In addition, the ionic contributions to the bonding increase for the Si—O and slightly decrease for the Si—O(C) bond compared to the parent silanol **2**. To put those values into perspective, we calculated the free model silanolates $[OSi\{OC(CF_3)_3\}_3]^-$, $[OSi(Ot-Bu)_3]^-$ as well as the smaller systems $[OSiH_3]^-$, $[OSiF_3]^-$ and $[OSi(OH)_3]^-$. The parameters observed for complex **3** and **6** are indeed very similar to those obtained for $[OSi(Ot-Bu)_3]^-$, $[OSiH_3]^-$ and $[OSi(OH)_3]^-$ in the AIM framework (Table S8). Inspection of the WBI and DI of the Si—O bond in **3** (0.86/0.47) and **6** (0.85/0.51) show increased values compared to the parent silanol **2** (0.70/0.38), but still smaller values than those obtained for free silanolates $[OSi(Ot-Bu)_3]^-$ (0.97/0.57), $[OSiH_3]^-$ (1.02/0.59) and $[OSi(OH)_3]^-$ (1.01/0.59, see Table 1 and Table S9). Interestingly, AIM analysis of the F-containing free silanolates $[OSiF_3]^-$ and $[OSi\{OC(CF_3)_3\}_3]^-$ leads to $\rho(r)_{bcp}$ values of 1.24 and $1.27 \text{ e}\text{\AA}^{-3}$ as well as $\nabla^2\rho(r)_{bcp}$ of 31.7 and $33.5 \text{ e}\text{\AA}^{-5}$. These values are even larger than for the Si⁺—O[−] bcp in Iwamoto's silanone R'₂Si⁺—O[−] (1.22/32.9; R'₂ = {C[C₆H₂(t-Bu)₂(OMe)]₂C₂H₄}).^[25] This observation prompted us to investigate whether the electronic distribution of the Si—O bond in a tetravalent silanolate is similar to that of a silanone. The WBI of the free $[OSi\{OC(CF_3)_3\}_3]^-$ anion of 1.15 as well as the DI of 0.60 are smaller than in Iwamoto's silanone (1.26/0.81). However, plotting the electron density as well as the Laplacian along the Si—O axis indeed reveals similarities between the $[OSi$

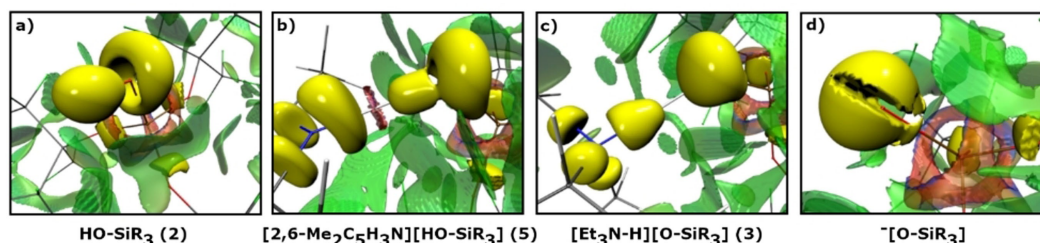


Figure 2. In transparent mode: NCI iso-surface at $s(r) = 0.6$ for the **2**, **5** and **3** molecules and the corresponding silanolate anion (R = OC(CF₃)₃), color coded with $\text{sign}(\lambda_2)\rho$ in a.u. Blue surfaces refer to attractive forces and red to repulsive forces. Green indicates weak van-der-Waals interactions; in solid-yellow: ELI-D localization domain representation of selected basins at iso-values of 1.46.

$\{\text{OC}(\text{CF}_3)_3\}^-$ anion and the silanone $\text{R}'_2\text{Si}^+-\text{O}^-$ (see Figures S48 and S49 of the Supporting Information).

In an attempt to quantify the degree of hyperconjugative interaction from the O-lone pairs to the Si-atom in the silanone on the one hand and the fluorinated silanolate $[\text{OSi}\{\text{OC}(\text{CF}_3)_3\}]^-$ on the other hand, we performed a Natural Localized Molecular Orbital (NLMO) Analysis.^[26] The NLMO analysis showed that in each case two NLMOs with p-lone pair character have significantly decreased parent NBO occupancies. In case of the silanolate $[\text{OSi}\{\text{OC}(\text{CF}_3)_3\}]^-$, the O atoms have parent NBO occupancies of 91.2% with contributions mainly from the Si atom (7.62%) and each give rise to SiO NLMO bond orders of 0.15, which make up 44.5% of the total NLMO bond order of 0.683 (see Table S10 for more details). In case of the silanone $\text{R}'_2\text{Si}^+-\text{O}^-$, the π -backdonation is stronger and contributes 55.5% to the total NLMO SiO bond order of 0.744. Overall, we conclude that the Si–O bonds in **3** and **6** show characteristics of those in free silanolates, such as $[\text{OSi}(\text{OH})_3]^-$ or $[\text{OSi}(\text{O}t\text{-Bu})_3]^-$, whereas the Si–O interaction in the free $[\text{OSi}\{\text{OC}(\text{CF}_3)_3\}]^-$ anion is similar to that usually observed in silanones, showing the possibility of mimicking the electronic distribution of a Si–O bond in silanones by tetravalent silanolates.

We finally calculated pK_a values of **2**, related silanols and some common acids in the gas phase and in MeCN (Figure 3).^[27] In MeCN, all previously known silanols show pK_a values from 29.8 ($\text{Si}(\text{OH})_4$) to 37.0 (Me_3SiOH) and are less acidic than common organic acids which in turn possess slightly smaller values ranging from 28.2 (phenol), 24.5 (acetic acid) to 21.3 (benzoic acid). In sharp contrast, **2** reveals the pK_a value of 17.4, which renders it to be significantly more acidic than all reference organic acids. The acidity of **2** in MeCN appears to be almost 20 orders of magnitude stronger than that for Me_3SiOH ($\text{pK}_a=37.0$), the least acidic silanol in the series. In the gas phase, the calculated acidity of **2** (229.2) even exceeds that of HCl (238.8).

In summary, we prepared the perfluorinated trialkoxysilanol $\{(\text{F}_3\text{C})_3\text{CO}\}_3\text{SiOH}$ (**2**), which can be regarded as a partial ester of orthosilicic acid, $\text{Si}(\text{OH})_4$. Due to the large number of fluorine atoms inducing charge separation, **2** is by more than 13 orders of magnitude more acidic than $\text{Si}(\text{OH})_4$ and by even more than

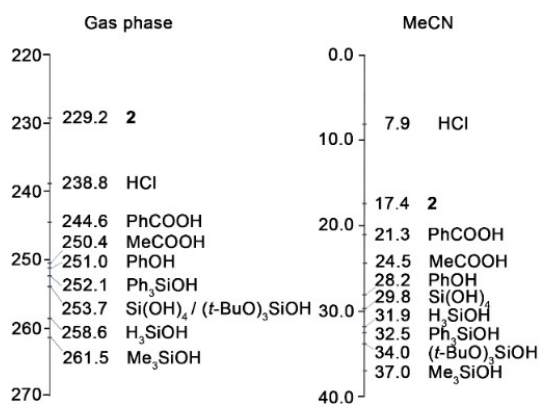


Figure 3. Calculated pK_a values of silanols and selected common acids in the gas phase and in MeCN

that compared to other previously known silanols. It is also significantly more acidic than common organic acids, such as benzoic acid, acetic acid or phenol. Despite the high intrinsic acidity, **2** shows no apparent tendency to undergo self-condensation to give siloxanes. In view of its easy preparation, **2** might be an ideal building block for the preparation of novel Lewis acids based upon highly fluorinated metallasiloxanes. The use in organocatalysis might be also envisaged.^[28]

Acknowledgements

The Deutsche Forschungsgemeinschaft (DFG) is gratefully acknowledged for financial support. The pK_a values were calculated within the Project 19-03-00755 supported by the Russian Foundation for Basic Research (RFBR). We thank Daniel Duvinage and Marian Olaru for the X-ray data collections and Peter Luger, Malte Hesse and Yu-Sheng Chen for their help with synchrotron measurements of $(t\text{-BuO})_3\text{SiOH}$ carried out at beamline 15-ID-B of ChemMatCARS at the Advanced Photon Source of the Argonne National Laboratories, Illinois, U.S.A. Open Access funding enabled and organized by Projekt DEAL.

Conflict of Interest

The authors declare no conflict of interest.

Keywords: acidity · Brønsted acid · fluorine · silanol · silicon

- [1] R. K. Iller, *The Chemistry of Silica*, Wiley, 1979.
- [2] a) P. D. Lickiss, *Adv. Inorg. Chem.* **1995**, *42*, 147; b) V. Chandrasekhar, R. Boomishankar, S. Nagendran, *Chem. Rev.* **2004**, *104*, 5847–5910.
- [3] L. L. Hench, J. K. West, *Chem. Rev.* **1990**, *90*, 33–72.
- [4] R. Murugavel, A. Vogt, M. W. Walawalker, H. W. Roesky, *Chem. Rev.* **1996**, *96*, 2205–2236.
- [5] K. J. Furdala, R. L. Brutchey, T. D. Tilley, *Top. Organomet. Chem.* **2005**, *16*, 69–115.
- [6] Deposition Number(s) CCDC 2086448 (1), 2086449 (3), 2086450 (3), 2086451 (5), 2086452 (6) and 2086273 (new non-disordered triclinic low-temperature modification (15 K) of $(t\text{-BuO})_3\text{SiOH}$, measured with synchrotron radiation at ChemMatCARS, Advanced Photon Source, USA, see Supporting Information) contain the supplementary crystallographic data for this paper. These data are provided free of charge by the joint Cambridge Crystallographic Data Centre and Fachinformationszentrum Karlsruhe Access Structures service.
- [7] J. Beckmann, D. Dakternieks, A. Duthie, M. L. Larchin, E. R. T. Tiekink, *Appl. Organomet. Chem.* **2003**, *17*, 52–62.
- [8] Consistently, the IR spectrum of **2** shows a sharp OH stretching vibration at $\tilde{\nu}=3117\text{ cm}^{-1}$. In solid $(t\text{-BuO})_3\text{SiOH}$, the OH stretching vibration of the silanol group being involved in hydrogen bonding was observed at $\tilde{\nu}=3398\text{ cm}^{-1}$. In CHCl_3 solution, there is an equilibrium between free ($\tilde{\nu}=3680\text{ cm}^{-1}$) and hydrogen-bonded $(t\text{-BuO})_3\text{SiOH}$ ($\tilde{\nu}=3391\text{ cm}^{-1}$). See Ref. [7].
- [9] a) R. West, R. H. Baney, *J. Am. Chem. Soc.* **1959**, *81*, 6145–6148; b) R. West, R. H. Baney, D. L. Powell, *J. Am. Chem. Soc.* **1960**, *82*, 6269–6272; c) R. Damrauer, R. Simon, M. Krempp, *J. Am. Chem. Soc.* **1991**, *113*, 4431–4435; d) M. Liu, N. T. Tran, A. K. Franz, J. K. Lee, *J. Org. Chem.* **2011**, *76*, 7186–7194.
- [10] There are very few alkali metal-free deprotonation reactions of silanols. a) R. F. Weitkamp, B. Neumann, H.-G. Stammler, B. Hoge, *Angew. Chem. Int. Ed.* **2020**, *59*, 5494–5499; *Angew. Chem.* **2020**, *132*, 5536–5541; b) R. F. Weitkamp, B. Neumann, H. G. Stammler, B. Hoge, *Chem. Eur. J.* **2021**, *27*, 915–920.

- [11] M. Igarashi, T. Matsumoto, F. Yagihashi, H. Yamashita, T. Ohhara, T. Hanashima, A. Nakao, T. Moyoshi, K. Sato, S. Shimada, *Nat. Commun.* **2017**, *8*, 140.
- [12] J. Beckmann, S. Grabowsky, *J. Phys. Chem. A* **2007**, *111*, 2011–2019.
- [13] a) J. Beckmann, A. Duthie, G. Reeske, M. Schürmann, *Organometallics* **2004**, *23*, 4630–4635; b) J. Beckmann, S. L. Jänicke, *Eur. J. Inorg. Chem.* **2006**, 3351–3358.
- [14] Due to the strengths of the hydrogen bonds, neither OH nor NH stretching vibrations were detectable by IR spectroscopy, most likely because the bands shifted to smaller wavenumbers and are too broad to be recognized from the baseline.
- [15] T. Steiner, *Angew. Chem. Int. Ed.* **2002**, *41*, 48–76; *Angew. Chem.* **2002**, *114*, 50–80.
- [16] A. Martens, P. Weis, M. C. Krummer, M. Kreuzer, A. Meierhöfer, S. C. Meier, J. Bohnenberger, H. Scherer, I. Riddellstone, I. Krossing, *Chem. Sci.* **2018**, *9*, 7058–7068.
- [17] a) A. C. Filippou, B. Baars, O. Chernov, Y. N. Lebedev, G. Schnackenburg, *Angew. Chem. Int. Ed.* **2014**, *53*, 565–570; *Angew. Chem.* **2014**, *126*, 576–581; b) I. Alvarado-Beltran, A. Rosas-Sánchez, A. Baceiredo, N. Saffon-Merceron, V. Branchadell, T. Kato, *Angew. Chem. Int. Ed.* **2017**, *56*, 10481–10485; *Angew. Chem.* **2017**, *129*, 10617–10621; c) D. Wendel, D. Reiter, A. Porzelt, P. J. Altmann, S. Inoue, B. Rieger, *J. Am. Chem. Soc.* **2017**, *139*, 17193–17198; d) R. Kobayashi, S. Ishida, T. Iwamoto, *Angew. Chem. Int. Ed.* **2019**, *58*, 9425–9428; *Angew. Chem.* **2019**, *131*, 9525–9528; e) S. Takahashi, K. Nakaya, M. Frutos, A. Baceiredo, N. Saffon-Merceron, S. Massou, N. Nakata, D. Hashizume, V. Branchadell, T. Kato, *Angew. Chem. Int. Ed.* **2020**, *59*, 15937–15941; *Angew. Chem.* **2020**, *132*, 16071–16075.
- [18] Compared to **2**, the ²⁹Si NMR chemical shifts (CDCl₃) of Si(OH)₄ (δ = –72.2 ppm) and (t-BuO)₃SiOH (δ = –90.4 ppm) are deshielded. See refs. 1 and 7.
- [19] a) V. Gutmann, *Coord. Chem. Rev.* **1976**, *18*, 225–255; b) M. Beckett, G. Strickland, *Polym. Commun.* **1996**, *37*, 4629–4631.
- [20] *Complementary Bonding Analysis* (S. Grabowsky; editor). De Gruyter: Berlin, Boston, **2021**.
- [21] P. A. Koutentis, M. Koyioni, S. S. Michaelidou, *Molecules* **2011**, *16*, 8992–9002.
- [22] a) M. Kohout, *Int. J. Quantum Chem.* **2004**, *97*, 651–658; b) M. Kohout, F. R. Wagner, Y. Grin, *Theor. Chem. Acc.* **2008**, *119*, 413–420.
- [23] E. R. Johnson, S. Keinan, P. Mori-Sánchez, J. Contreras-García, A. J. Cohen, W. Yang, *J. Am. Chem. Soc.* **2010**, *132*, 6498–6506.
- [24] R. W. F. Bader *Atoms in Molecules. A Quantum Theory*; Cambridge University Press: Oxford U.K., **1991**.
- [25] For better comparison, a single-point calculation was performed at the B3PW91/cc-pVTZ level of theory taking the reported coordinates from Ref. [17]d. For further details, see the Supporting Information.
- [26] Eric D. Glendening, Clark R. Landis, Frank Weinhold, *WIREs Comput. Mol. Sci.* **2012**, *2*, 1–42.
- [27] a) R. Kather, E. Rychagova, P. Sanz Camacho, S. E. Ashbrook, J. D. Woollins, L. Robben, E. Lork, S. Ketkov, J. Beckmann *Chem. Commun.* **2016**, *52*, 10992–10995; b) M. Olaru, M. F. Hesse, E. Rychagova, S. Ketkov, S. Mebs, J. Beckmann, *Angew. Chem. Int. Ed.* **2017**, *56*, 16490–16494; *Angew. Chem.* **2017**, *129*, 16713–16717. For further details, see the Supporting Information.
- [28] a) N. T. Tran, T. Min, A. K. Franz, *Chem. Eur. J.* **2011**, *17*, 9897–9900; b) A. M. Hardman-Baldwin, A. E. Mattson, *ChemSusChem* **2014**, *7*, 3275–3278; c) J. Pérez-Pérez, U. Hernández-Balderas, D. Martínez-Otero, V. Jancik, *New J. Chem.* **2019**, *43*, 18525–18533.

Manuscript received: September 1, 2021

Accepted manuscript online: September 22, 2021

Version of record online: October 14, 2021